

# Magnesium ion transport in poly(ethylene oxide)-based polymer electrolyte containing plastic-crystalline succinonitrile

Jyoti Sharma · S. A. Hashmi

Received: 28 January 2013 / Revised: 15 April 2013 / Accepted: 17 April 2013 / Published online: 9 May 2013  
© Springer-Verlag Berlin Heidelberg 2013

**Abstract** A new composition of magnesium (Mg)-ion-conducting polymer electrolyte comprising poly(ethylene oxide) (PEO) complexed with Mg trifluoromethanesulfonate (Mg triflate or  $\text{Mg}(\text{Tf})_2$ ) containing different amounts of a nonionic plastic crystal succinonitrile (SN) has been prepared and characterized. High polarity and rotational disorder of the SN molecules in the plastic-crystalline phase, supports the enhancement of ionic conductivity of the PEO- $\text{Mg}(\text{Tf})_2$  complex system, showing a maximum room temperature ionic conductivity of  $\sim 6 \times 10^{-4} \text{ S cm}^{-1}$  observed with the addition of 50 wt.% of SN. X-ray diffraction, optical microscopy, and differential scanning calorimetry suggest a substantial structural modification, decrease in crystallinity, and various interactions in the polymer electrolyte components due to addition of SN. The cyclic voltammetry, impedance, and dc polarization studies confirm the Mg-ion conduction in the PEO complex. The electrochemical potential window of the electrolyte, observed from the linear sweep voltammetry, is determined to be  $\sim 4.1 \text{ V}$ . The performance characteristics of the SN-incorporated polymer electrolyte system indicate their potential applicability as electrolytes in ionic devices including Mg batteries.

**Keywords** Polymer electrolyte · Succinonitrile · Ionic conductivity · Magnesium-ion conduction

## Introduction

In recent years, development of compact, light-weight, cost-effective, and high-energy density batteries are in great

demand [1]. Rechargeable lithium (Li) batteries have been studied for a long time [1–12] because of the high electrochemical reduction potential of Li ( $-3.04 \text{ V}$  with respect to standard hydrogen electrode) and high volumetric capacity ( $2,062 \text{ mA h cm}^{-3}$ ). But the passivation layer formation at the electrode–electrolyte interfaces and dendritic growth of Li in the electrolyte region are some of the problems which limit the shelf life and cyclic stability of Li batteries [1, 2]. Recently, the electrochemistry of sodium, zinc, and magnesium (Mg) has been investigated and found these metals as suitable alternatives of the Li anode for the development of the rechargeable batteries [13–20]. Particularly, the Mg-based rechargeable batteries are under the current investigations because of their performance capabilities close to the Li-based systems [17–20]. The ionic radius of  $\text{Mg}^{2+}$  ions ( $r_{\text{Mg}^{2+}} = 0.072 \text{ nm}$ ) is comparable to that of Li ( $r_{\text{Li}^+} = 0.076 \text{ nm}$ ). Apart from the fact that Mg metal is stable, abundant, and more cost effective than Li, it possesses high volumetric capacity of  $3,833 \text{ mA h cm}^{-3}$  and electrochemical reduction potential ( $-2.37 \text{ V}$  with respect to standard hydrogen electrode) [20]. These properties of Mg metal are attractive enough to develop the Mg batteries in combination with the suitable electrolyte and cathode materials.

One of the key factors which decides the lifetime and cyclic performance of a battery is a suitable choice of electrolyte which provides the sufficient control at the interfaces and medium for the ions for high mobility. Batteries using liquid electrolytes have been known for a long time; however, they are faced with several problems including leakage, flammability and toxicity of the electrolyte, corrosion of the electrodes during multiple charge–discharge cycling, bulky battery design, etc. [21]. The ion-conducting polymers as electrolytes have potential to overcome these problems because of their solid-like nature, improved electrochemical and thermal stability, absence of leakage, miniaturization, and moldability for better transportability [22, 23].

J. Sharma · S. A. Hashmi (✉)  
Department of Physics and Astrophysics, University of Delhi,  
Delhi 110007, India  
e-mail: sahashmi@physics.du.ac.in

Extensive studies have been carried on solid polymer electrolytes/complexes consisting of poly(ethylene oxide) (PEO) and alkali metal salts for solid-state batteries. PEO has the ability to coordinate effectively with salt cations and offers excellent dimensional stability in the form of free-standing films with good ionic conductivity [22, 23]. Most of the reported PEO-based electrolytes comprise Li salts which are useful electrolytes in Li batteries [2, 24]. Few PEO-Mg salts complexes have been reported which are predominantly anionic conductors with negligible  $\text{Mg}^{2+}$ -ion conductivity because of the strong electrostatic interaction between  $\text{Mg}^{2+}$  ion and ether oxygen of PEO [22, 25]. Some efforts have been devoted to enhance  $\text{Mg}^{2+}$ -ion transport in PEO/Mg salt complexes, to employ them in Mg batteries, by incorporating plasticizers like ethylene carbonate, propylene carbonate, etc. [26]. Recently, Kumar et al. [27] reported a substantial enhancement in  $\text{Mg}^{2+}$ -ion transport in PEO/Mg triflate system due to the addition of an ionic liquid. The ionic liquid incorporation leads to the additional properties of polymer electrolytes including non-flammability, nonvolatility, and high thermal and electrochemical stability [27]. However, the main drawback of such ionic liquid-based polymer electrolytes is the complexities in ionic conduction owing to the mobility of component ions of the ionic liquids [28].

Recently, some polymer-based electrolytes have been investigated using plastic-crystalline material-like succinonitrile (SN) which acts as solid plasticizer [29–34]. The SN is a nonionic plastic crystal which acts as a polar solvent having high dielectric constant ( $\sim 55$  at  $25\text{ }^\circ\text{C}$ ) [35]. The high dielectric constant value of SN ensures its ability to dissociate various salts for ionic conduction. Its plastic character before its melting point, due to the presence of impurity *trans* isomers, provides the vacancies for ion transport and makes the polymer network flexible which improves the electrical properties of polymer electrolytes. Polymer electrolytes containing the plastic crystal SN have attractive features including vanishingly small vapor pressure (hence the electrolyte evaporation can be avoided) and reduced flammability which reduces the safety concern.

In the present work, we report a novel composition of  $\text{Mg}^{2+}$ -ion-conducting PEO-based polymer electrolyte complexed with Mg trifluoromethanesulfonate, i.e.,  $\text{Mg}(\text{Tf})_2$  incorporated with the plastic-crystalline SN as plasticizer in solid phase. Various techniques such as X-ray diffraction (XRD), optical microscopy, differential scanning calorimetry (DSC), thermogravimetric analysis (TGA), impedance analysis, and cyclic/linear sweep voltammetry have been used to characterize and optimize the polymer electrolytes. It has been observed that the polymer electrolyte PEO/ $\text{Mg}(\text{Tf})_2$ /SN is a Mg-ion-conducting, free-standing film, useful as a separator/electrolyte in Mg batteries.

## Experimental

### Preparation of materials

PEO (average molecular weight,  $\sim 6 \times 10^5$ ), Mg trifluoromethane sulfonate  $\text{Mg}(\text{Tf})_2$  (purity, 97 %), and SN (purity, 99 %) were obtained from Sigma-Aldrich. The PEO and salt  $\text{Mg}(\text{Tf})_2$  were vacuum dried at temperatures of 30 and  $100\text{ }^\circ\text{C}$ , respectively. SN was further purified by recrystallization process. The polymer electrolyte films were prepared by “solution-cast” method. PEO and different amounts of SN (with respect to the weight of PEO) were separately dissolved in a common solvent acetonitrile by stirring them magnetically at room temperature for about 24 h. The appropriate amounts of  $\text{Mg}(\text{Tf})_2$  were added to the SN solutions and stirred for  $\sim 12$  h to obtain homogeneous solutions. These solutions were then mixed with the PEO/acetonitrile solutions and stirred magnetically further for  $\sim 12$  h. The EO/ $\text{Mg}^{2+}$  ratio was kept at  $\sim 20$  for all the compositions. These solutions were then poured in Teflon Petri dishes, and the common solvent acetonitrile was allowed to evaporate slowly at room temperature for 4–5 days. After complete drying, free-standing polymer electrolyte films were peeled off from the dishes. Finally, these films were dried rigorously under vacuum ( $\sim 10^{-3}$  Torr) at room temperature for 2–3 days and stored in argon atmosphere to avoid adsorption of moisture. Binary mixtures of 5 mol% of  $\text{Mg}(\text{Tf})_2$  in SN and PEO/SN (2:1 (w/w) ratio) were also prepared using the above method for comparison. The composition of the polymer electrolytes will be referred to as  $\text{PEO}_{20}\cdot\text{Mg}(\text{Tf})_2+x$  wt.% SN in rest of the text.

The circular discs of Mg electrodes (area,  $\sim 1.2\text{ cm}^2$ ) were prepared by pressing the Mg powder (Aldrich) at 4 tons  $\text{cm}^{-2}$  to use them as reversible electrodes. These discs were polished with successive grades of emery papers for a smooth finishing then washed thoroughly in acetone and dried. The stainless steel (SS) sheets (Alfa Aesar, grade 304) were used as blocking electrodes.

### Physical characterization

Thermal studies of the polymer electrolyte films were carried out by DSC and TGA. DSC measurements were performed under static nitrogen atmosphere using a calorimeter of TA Instruments (model, Q100). The samples were loaded in low-mass aluminum pans, and measurement temperatures were taken from  $-90$  to  $250\text{ }^\circ\text{C}$  at a heating rate of  $10\text{ }^\circ\text{C min}^{-1}$ . Each sample was first cooled from room temperature to  $-90\text{ }^\circ\text{C}$  by a cooling rate of  $3\text{ }^\circ\text{C min}^{-1}$  and was equilibrated at this temperature for 10 min before recording the DSC plot in the heating cycle. TGA was carried

out using a Perkin Elmer TGA system (TGA-7) in dry nitrogen atmosphere from room temperature to 480 °C at the same heating rate mentioned above.

Comparative changes in crystalline/amorphous textures in the electrolyte films were monitored by XRD at room temperature using an X-ray diffractometer (model, D8 DISCOVER, Bruker) at a scan rate of 2°/min in a Bragg angle ( $2\theta$ ) range from 10° to 60°. Morphological changes in the polymer electrolytes were observed using Nomarsky contrast optical microscope (model, MX61, Olympus, Japan).

Electrochemical impedance spectroscopic (EIS) studies were carried out to evaluate the ionic conductivity using LCR Hi-TESTER (model, 3522–50, HIOKI, Japan) in a frequency range from 1 Hz to 100 kHz with signal amplitude of 10 mV. The conductivity measurements were performed by sandwiching the electrolyte films between two symmetrical SS sheets. The temperature dependence of the ionic conductivity was recorded over the temperature range from 28 to 100 °C. The electrochemical studies were performed by cyclic voltammetry (CV) and linear sweep voltammetry (LSV) using an electrochemical analyzer (model, 608C, CH Instruments, USA). The dc polarization measurements were carried out for two cells with the symmetrical configuration using SS and Mg electrodes, namely, SS|electrolyte|SS and Mg|electrolyte|Mg. These cells were polarized by applying a dc voltage of 0.75 V.

## Results and discussion

### Thermal studies: DSC and TGA

DSC curves of pure PEO and SN, binary mixtures PEO/SN and SN/Mg(Tf)<sub>2</sub>, and PEO<sub>20</sub>·Mg(Tf)<sub>2</sub> polymer complexes added with different amounts of SN (varying from 0 to 50 wt.%), recorded from –90 to 250 °C, are shown in Fig. 1. Pure PEO shows an endothermic melting peak at ~67 °C (Fig. 1a). Pure SN shows a plastic-crystalline phase between –38 (the transition from normal to plastic-crystalline phase ( $T_{pc}$ )) and 57 °C (melting point of SN ( $T_m$ )) (Fig. 1b) [36]. The abrupt peaks observed for pure SN beyond 150 °C (Fig. 1b) are due to the fast evaporation of SN. On the addition of Mg(Tf)<sub>2</sub>, the melting peak of SN has been decreased to ~33 °C (Fig. 1d), while  $T_{pc}$  remains unaffected. The decrease in  $T_m$  is due to the solvating ability of SN [37] which indicates the Mg–salt interaction with SN.

When SN is added to pure PEO (with a weight ratio of 1:2), only one endothermic peak is observed at a temperature of ~60 °C. Normal to plastic-crystalline phase transition peak of SN at  $T_{pc}$  ~–38 °C completely disappears (Fig. 1c). The melting peak of PEO ( $T_m$ , ~67 °C) reduces to ~60 °C and possibly overlaps with the melting peak of SN, showing a broader peak (Fig. 1c). These changes indicate the

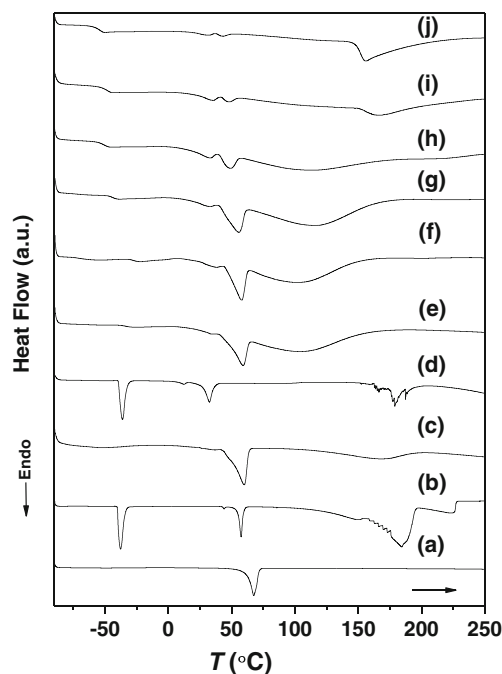


**Fig. 1** DSC curves of pure PEO film (a), pure SN (b), PEO/SN (2:1, w/w; c), Mg(Tf)<sub>2</sub>/SN (5 mol% Mg(Tf)<sub>2</sub> in SN; d), and PEO<sub>20</sub>·Mg(Tf)<sub>2</sub>+xwt.% SN polymer electrolyte systems for x=0 (e), 5 (f), 10 (g), 30 (h), 40 (i), and 50 (j)

possible donor–acceptor interaction of ether oxygen of PEO with N≡C group of SN [30]. Such interaction has also been evidenced on the basis of FTIR studies reported earlier [38–40].

When PEO is complexed with Mg(Tf)<sub>2</sub>, its melting peak is lowered to ~59 °C (Fig. 1e), and as the SN concentration increases from 5 to 50 wt.%, the intensity of this peak decreases (Fig. 1f–j), which shows the decrease in crystalline nature of PEO. Different parameters, glass-transition temperature ( $T_g$ ),  $T_m$ ,  $\Delta H_m$ , and degree of crystallinity, evaluated from the melting peaks of PEO for all the compositions, are listed in Table 1. A substantial decrease in the degree of crystallinity due to the addition of SN in the PEO<sub>20</sub>·Mg(Tf)<sub>2</sub> complex can be seen from Table 1. The decrease in crystallinity (hence increase in the amorphous fraction) in polymer electrolyte films has been observed due to the localization of the PEO chains in SN domain. The decrease in the crystalline nature of PEO–Mg salt complexes due to the addition of SN are discussed in XRD studies also in the following section.

An endothermic broad hump has also been observed between 65 and 170 °C for the PEO<sub>20</sub>·Mg(Tf)<sub>2</sub> system which is assigned to the amorphous phase of PEO complex with Mg salt [27]. As the SN concentration increases in PEO<sub>20</sub>·Mg(Tf)<sub>2</sub> complex, the intensity of this broad hump decreases and shifts towards the higher temperature range.

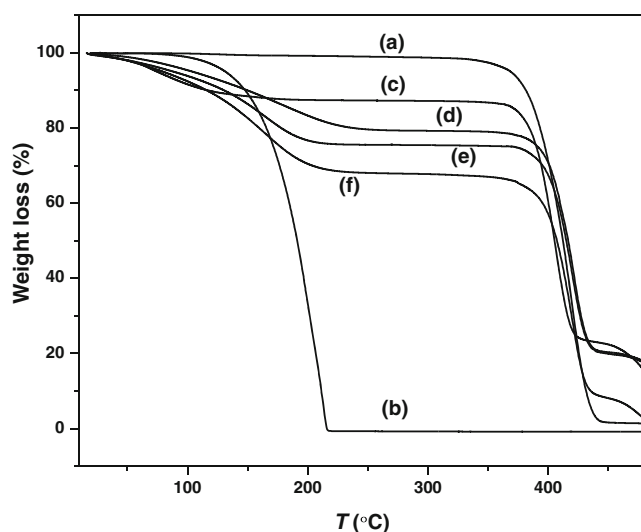
A step change, owing to the  $T_g$  is distinctly observed in polymer electrolyte films containing 5–10 wt.% of SN at

**Table 1** Different parameters ( $T_g$ ,  $T_m$ ,  $\Delta H_m$ , and percent crystallinity) determined from DSC studies

Compositions	$T_g$ (°C)	$T_m$ (°C)	$\Delta H_m$ (J g <sup>-1</sup> )	Crystallinity (%)
Pure PEO	–	67	170.2	90
PEO+SN (2:1, w/w)	–	60	142.5	75
PEO <sub>20</sub> ·Mg(Tf) <sub>2</sub>	–	59	50.8	27
PEO <sub>20</sub> ·Mg(Tf) <sub>2</sub> +5 wt.% SN	–27.42	58	52.6	28
PEO <sub>20</sub> ·Mg(Tf) <sub>2</sub> +10 wt.% SN	–44.72	55	49.3	26
PEO <sub>20</sub> ·Mg(Tf) <sub>2</sub> +20 wt.% SN	–47.02	51	32.9	17
PEO <sub>20</sub> ·Mg(Tf) <sub>2</sub> +30 wt.% SN	–51.26	48	22.3	12
PEO <sub>20</sub> ·Mg(Tf) <sub>2</sub> +40 wt.% SN	–49.31	47	7.6	4
PEO <sub>20</sub> ·Mg(Tf) <sub>2</sub> +50 wt.% SN	–55.26	43	3.5	2

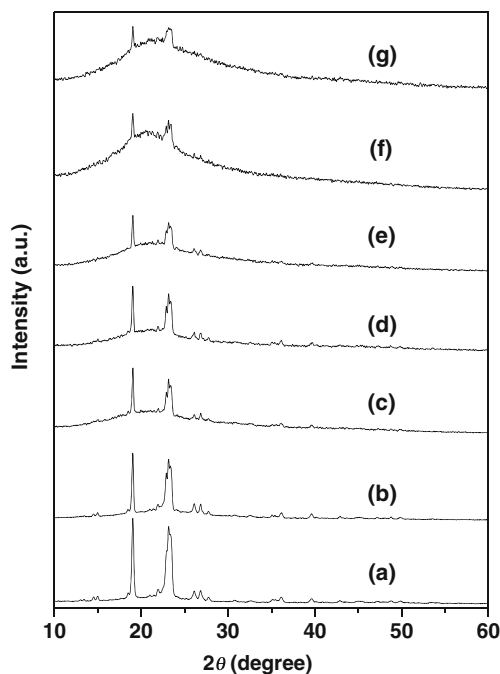
about –27 °C (with onset of  $T_g$  at –32 °C). On increasing the content of SN, this step change shifts towards the lower temperature side (Fig. 1g–j). This down shifting of the  $T_g$  shows the plasticizing effect of SN, responsible for increasing the flexibility of the polymeric films.

TGA curves for pure PEO and SN, and the PEO<sub>20</sub>·Mg(Tf)<sub>2</sub> complexes added with different amounts of SN over the temperature range from room temperature to 480 °C are shown in Fig. 2. The host polymer PEO shows no weight loss indicating its thermal stability up to ~340 °C. The SN, which is an adduct in the present polymer electrolyte system, is stable up to ~100 °C and evaporates fully at 216 °C. The thermal stability of SN is observed up to 100 °C in the present condition of TGA measurement, however, the isothermal TGA study indicates the stability up to 80 °C only, as reported by Echeverri et al. [38]. The polymer electrolytes containing different amounts of SN show marginal weight loss of (~4–7 wt.%) up to 100 °C, which may be due to the presence of moisture-sensitive salt Mg(Tf)<sub>2</sub>.

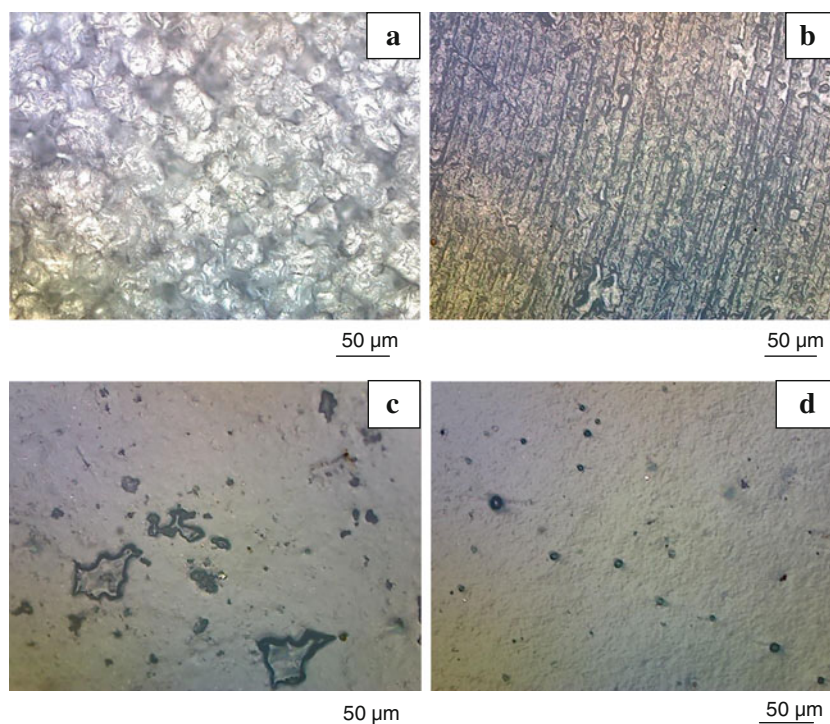
**Fig. 2** TGA curves of pure PEO film (a), pure SN (b), and PEO<sub>20</sub>·Mg(Tf)<sub>2</sub>+xwt.% SN polymer electrolyte systems for x=0 (c), 30 (d), 40 (e), and 50 (f)

Structural studies: XRD and optical microscopy

XRD and optical microscopic studies have been performed to investigate the possible changes in semi-crystalline nature of PEO<sub>20</sub>·Mg(Tf)<sub>2</sub> complexes due to the addition of SN. Fig. 3 shows the XRD patterns of PEO (pure), PEO/SN blend, PEO<sub>20</sub>·Mg(Tf)<sub>2</sub> complex, and PEO complexes containing different amounts of SN. The XRD peaks, observed at  $2\theta$  ~19.0°, 23.1°, 26.1°, 26.9°, and 27.8° indicate the semi-crystalline nature of PEO. The addition of SN to PEO does not affect its semi-crystalline nature; however, no additional peak associated with SN is observed (Fig. 3b). It may be noted that the pure SN shows two characteristic peaks at ~20° and 28°, as reported in literature [29, 41]. This indicates that the SN is fully dissolved in PEO [41]. A low-intensity broad hump appears between 15° and 30°, when Mg(Tf)<sub>2</sub> is added

**Fig. 3** XRD patterns of pure PEO film (a), PEO/SN (2:1, w/w) (b) and PEO<sub>20</sub>·Mg(Tf)<sub>2</sub>+xwt.% SN polymer electrolyte systems for x=0 (c), 10 (d), 30 (e), 40 (f), and 50 (g)

**Fig. 4** Optical micrographs of pure PEO (a) and  $\text{PEO}_{20}\cdot\text{Mg}(\text{Tf})_2+x\text{wt.}\%$  SN polymer electrolyte systems for  $x=0$  (b), 5 (c), and 30 (d)



in PEO to prepare the PEO complex (Fig. 3c). On the addition of SN in  $\text{PEO}\cdot\text{Mg}(\text{Tf})_2$  complex, the intensity of the broad peak increases with increasing content of SN. This indicates the enhancement of amorphous nature of the polymer electrolytes. It may be noted that even after the addition of substantial amount of SN, the sharp crystalline peaks of PEO still exist. This shows that the partial crystalline nature of the PEO persists even after the incorporation of SN. The enhancement in the amorphous nature increases the flexibility and hence the segmental motion of polymeric chains, which thereby

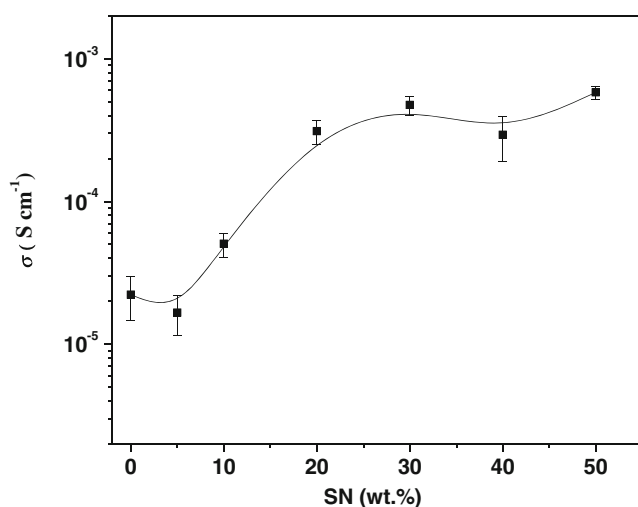


**Fig. 5** Electrical conductivity variation of  $\text{PEO}_{20}\cdot\text{Mg}(\text{Tf})_2+x\text{wt.}\%$  SN polymer electrolyte systems as a function of SN content recorded at room temperature

increases the ion mobility and hence ionic conductivity. The enhancement in amorphous character (i.e., decrease in crystallinity) has also been observed in DSC studies, discussed in the previous section.

Gross morphological changes have been observed in PEO texture due to the addition of Mg salt and different amounts of SN. Figure 4 shows the optical micrographs of the pure PEO,  $\text{PEO}_{20}\cdot\text{Mg}(\text{Tf})_2$  complex, and  $\text{PEO}_{20}\cdot\text{Mg}(\text{Tf})_2$  complexes added with 5 and 30 wt.% SN. Pure PEO shows the spherulitic structure with dark boundaries which indicates its semi-crystalline nature. The spherulitic texture disappears and a completely different texture is observed when PEO is complexed with Mg salt, as shown in Fig. 4b. Regular arrays of polymer-complex strands are observed, separated by linear dark regions. On the addition of different amounts of SN, almost flat surfaces are observed, which indicates the interacting role of SN with PEO system. The dark islands shown in the micrographs (Fig. 4c, d) are possibly the regions where PEO could not find sufficient amount of SN for interaction. The spots are less in number and smaller in sizes when the SN content is more (Fig. 4d).

#### Ionic conductivity

The variation in room-temperature ( $\sim 26^\circ\text{C}$ ) ionic conductivity of the polymer electrolyte with respect to the content of SN is depicted in Fig. 5. A gradual increase in conductivity is observed when SN is added to the  $\text{PEO}_{20}\cdot\text{Mg}(\text{Tf})_2$  complex and get almost saturated beyond  $\sim 20$  wt.% of SN. An optimum conductivity of  $\sim 6 \times 10^{-4} \text{ S cm}^{-1}$  has been

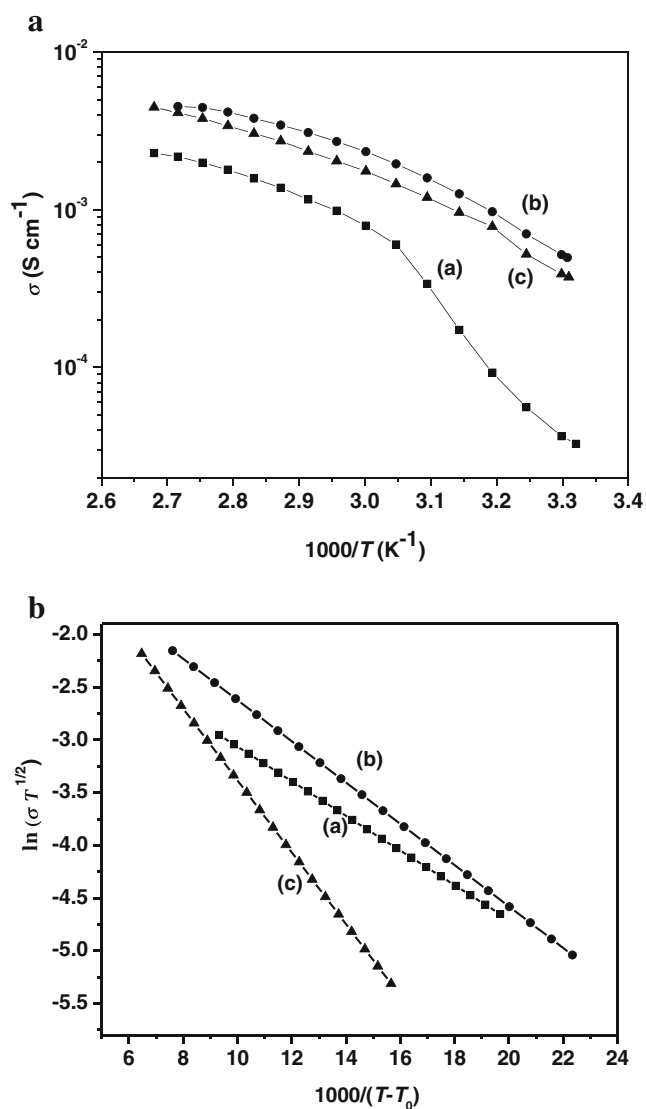


**Fig. 6** **a** The temperature dependence of electrical conductivity of PEO<sub>20</sub>:Mg(Tf)<sub>2</sub>+*x* wt.% SN polymer electrolyte systems for *x*=10 (a), 30 (b), and 50 (c). **b** The corresponding  $\ln(\sigma T^{1/2})$  vs.  $1/(T-T_0)$  plots

achieved on the addition of ~50 wt.% SN. On further addition of the SN beyond 50 wt.%, the electrolyte loses its dimensional stability, showing a glue-like nature. The initial increase in the ionic conductivity (by more than one order of magnitude) is associated with the ionic conduction in the structurally modified polymeric network of PEO due to the addition of the plastic-crystalline SN molecules. The following important points can be considered responsible for the enhancement in the ionic conductivity:

1. The Mg salt gets slightly dissociated, when added to the PEO network of dielectric constant of ~5 to form PEO-Mg salt complexes. The dissociated Mg<sup>2+</sup> cations have tendency to coordinate with ether oxygen of PEO via Lewis acid–base interactions

**Table 2** *A*, *B*, and *T*<sub>0</sub> values for PEO<sub>20</sub>:Mg(Tf)<sub>2</sub> complex with 10, 30, and 50 wt.% SN determined by nonlinear least square fitting of conductivity data to VTF equation

SN content <i>x</i> (wt.%)	<i>T</i> <sub>0</sub> (K)	<i>A</i> (S cm <sup>-1</sup> K <sup>1/2</sup> )	<i>B</i> (eV)
10	275	0.24	0.010
30	255	0.51	0.012
50	235	1.02	0.021

[22]. Such interactions/coordination are strong enough, leading to almost no contribution of Mg<sup>2+</sup> ions in total ionic conductivity. As a result, most of the PEO-Mg salt complexes are reported to be anionic conductors [22, 25]

2. The Gutmann donor number of the nitrile group of SN is lower (~15) as compared with that for PEO (~22) and hence the nitrile group of SN has also a tendency to coordinate with ether oxygen of PEO [30, 42]. The interaction of the nitrile group of SN with ether oxygen of PEO has also been evidenced from FTIR studies, as mentioned earlier [38–40]. Thus, the formation of some PEO–SN complexes is also possible in the present polymer electrolyte system PEO<sub>20</sub>:Mg(Tf)<sub>2</sub>/SN.
3. In the new environment of PEO/SN network of high dielectric constant (the dielectric constant of SN being 55 [35, 42]), a further charge separation of the Mg salts would occur. As a result, Mg<sup>2+</sup> cations (along with the Tf<sup>-</sup> anions) would become freer for conduction. Thus, the PEO/SN/Mg(Tf)<sub>2</sub> polymer electrolytes become Mg<sup>2+</sup> ion conducting.

The temperature dependence of ionic conductivity of the PEO<sub>20</sub>:Mg(Tf)<sub>2</sub> complexes added with different amounts of SN for the temperature range from 28 to 100 °C is presented in Fig. 6a. The “ $\sigma$  vs.  $1/T$ ” plot for the polymer electrolyte

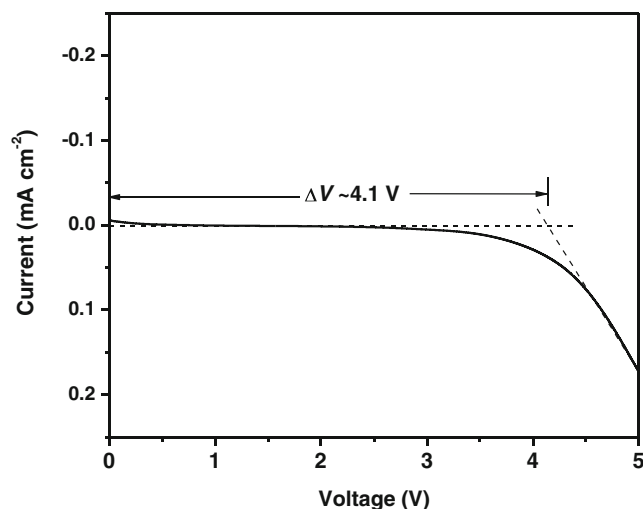


**Fig. 7** Linear sweep voltammogram of SS|polymer electrolyte|Mg cell at the scan rate of 5 mV s<sup>-1</sup>

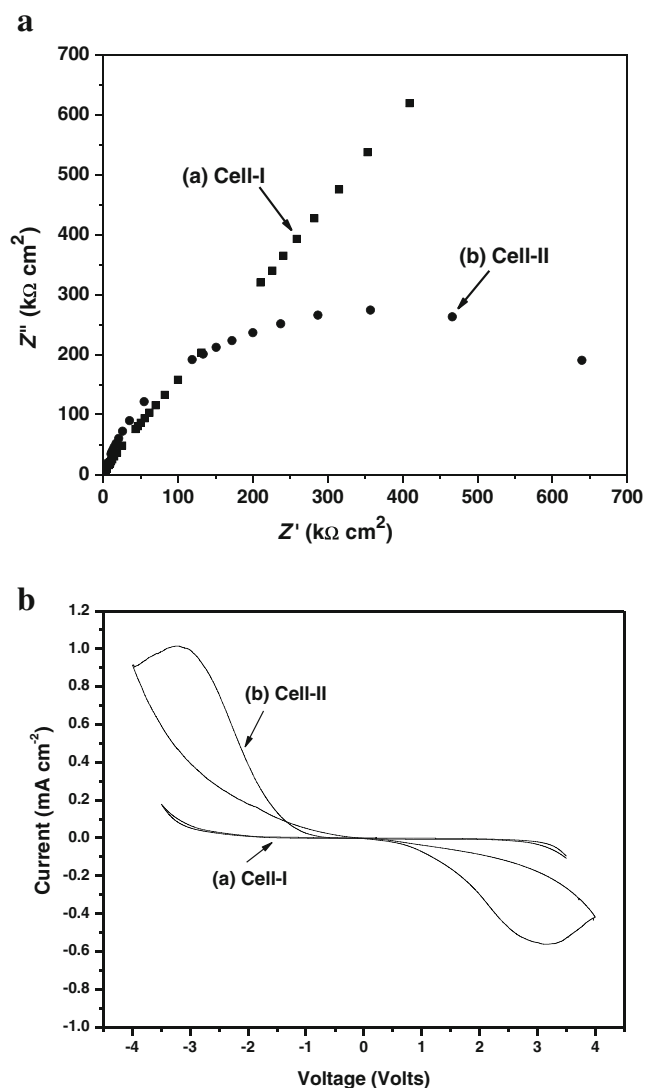


**Fig. 8** **a** Complex impedance plots for *a* cell-I: SS|polymer electrolyte|SS and *b* cell-II: Mg|polymer electrolyte|Mg. **b** Cyclic voltammograms of *a* cell-I: SS|polymer electrolyte|SS and *b* cell-II: Mg|polymer electrolyte|Mg, recorded at room temperature at the scan rate of  $5\text{ mV s}^{-1}$

with 10 wt.% of SN depicts a typical behavior of PEO-based electrolytes. The material indicates steep increase in conductivity around melting temperature  $T_m$  ( $67\text{ }^\circ\text{C}$ ) up to the temperature  $70\text{ }^\circ\text{C}$ , beyond that  $\sigma$  vs.  $1/T$  plot shows a curved nature (Fig. 6a (a)). The curved nature of conductivity variations are observed for the larger range of temperature (from 28 to  $100\text{ }^\circ\text{C}$ ) when a substantial amount of SN (30–50 wt.%) is added to PEO-Mg(Tf)<sub>2</sub> system (Fig. 6a (b, c)). The curved variation of  $\sigma$  vs.  $1/T$  plot indicates the non-Arrhenius Vogel–Tamman–Fulcher (VTF) behavior, expressed as:

$$\sigma = AT^{-\frac{1}{2}} \exp\left(\frac{-B}{T - T_0}\right)$$

where the parameter  $B$  is associated with the rate at which viscosity changes with temperature,  $A$  is a pre-exponential

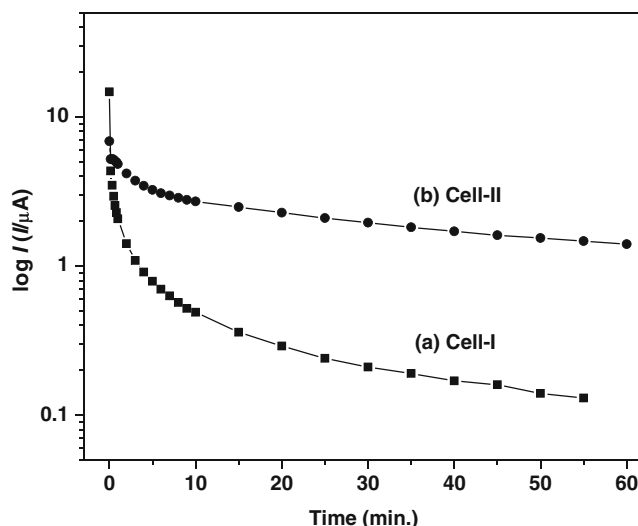


**Fig. 9** Polarization curves for *a* cell-I: SS|polymer electrolyte|SS, *b* cell-II: Mg|polymer electrolyte|Mg, at room temperature

factor, i.e., the conductivity at infinitely high temperature and  $T_0$  is the equilibrium glass transition temperature close to the  $T_g$  value. The  $\ln(\sigma T^{1/2})$  vs.  $1/(T - T_0)$  plot for each polymer electrolyte has been drawn and found to be linear (Fig. 6b). These linear variations are fitted using nonlinear least square fitting to evaluate the parameters  $A$ ,  $B$ , and  $T_0$ . These parameters are listed in Table 2. The polymer electrolytes with 30–50 wt.% of SN exhibit ionic conductivity more than  $5 \times 10^{-4}\text{ S cm}^{-1}$  at room temperature and  $\sim 5 \times 10^{-3}\text{ S cm}^{-1}$  at  $\sim 100\text{ }^\circ\text{C}$ , showing a good substitute of liquid electrolytes for the application in Mg batteries for a wider temperature span.

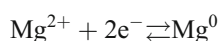
### Electrochemical properties

The electrochemical stability window (i.e., working voltage range) for a typical composition of the polymer electrolyte film with 50 wt.% SN has been evaluated using LSV. The LSV response was recorded on the cell: SS|polymeric electrolyte|Mg using SS as a working electrode and Mg as both the counter and reference electrodes. It can be seen from Fig. 7 that the film has been electrochemically stable up to  $\sim 4.1\text{ V}$  [43] which is a sufficient range for electrochemical applications, particularly for Mg batteries.

To confirm the Mg-ion conduction in the polymer electrolyte system, the EIS, CV, and dc polarization studies have been performed on symmetrical cells: SS|electrolyte film|SS (cell-I) and Mg|electrolyte film|Mg (cell-II) with a typical composition of the polymer electrolyte PEO<sub>20</sub>·Mg(Tf)<sub>2</sub>+ 50 wt.% SN. The polymeric film was in contact with a SS in cell-I as a blocking electrode, whereas the pellets of Mg powder were used as reversible (nonblocking) electrodes in cell-II. The comparative EIS plots for cell-I and cell-II, recorded at room temperature are depicted in Fig. 8(a).

The impedance response of cell-I shows a steep rise of imaginary impedance ( $Z''$ ) with respect to real impedance ( $Z'$ ) in the lower frequency range, indicating the ion blocking nature of SS electrodes. A well-defined semicircular curve is observed for cell-II, indicating the reversibility of Mg/Mg<sup>2+</sup> couple at the electrolyte–electrode interfaces. This confirms the Mg<sup>2+</sup> ion conduction in the polymer electrolyte film.

The conduction of Mg<sup>2+</sup> ions in the polymer electrolyte film is further confirmed from CV measurements. Figure 8b shows the CV curves for cell-I (with SS electrodes) and cell-II (with Mg electrodes) at the scan rate of 5 mV s<sup>-1</sup>. The cathodic and anodic current peaks are distinctly observed for cell-II, whereas no such features are present in the case of cell-I in the same potential range. These peaks correspond to equilibrium attained by Mg<sup>2+</sup> ions at the interfaces following the reversible reaction:



that is, the cathodic deposition and anodic oxidation of Mg take place at the electrode–electrolyte interfaces.

In order to further confirm the Mg<sup>2+</sup> ion conduction in the polymer electrolyte film, the polarization experiments have been performed on the cells: cell-I (SS/SS) and cell-II (Mg/Mg). The polarization (current vs. time) curves for the cells are shown in Fig. 9. For the cell-I (with SS electrodes), the polarization current decreases rapidly, and it approaches to a value close to zero. The ionic transport number ( $t_{\text{ion}}$ ), has been evaluated to be >0.99 [44]. The value of  $t_{\text{ion}}$  and the variation of polarization curve indicate the predominant ionic conduction in the electrolyte. For the cell-II (with the reversible Mg electrodes), the current steeply decreases initially and a steady-state value is reached after a sufficient time of polarization. The steady state is obtained due to constant supply of Mg<sup>2+</sup> ions from positive electrode and their dissolution in the negative Mg electrode. This further confirms the conduction of Mg<sup>2+</sup> ions through the polymer electrolyte film.

## Conclusions

A PEO-based Mg<sup>2+</sup>-ion-conducting polymer electrolyte complexed with Mg triflate containing a nonionic plastic-crystalline solid-phase plasticizer SN has been prepared and characterized. The semi-crystalline nature of the electrolyte materials with predominant amorphous character is evidenced from XRD, optical microscopy and DSC studies. The free-standing film of PEO complex with ~50 wt.% of SN offers optimum ionic conductivity of  $\sim 6 \times 10^{-4}$  S cm<sup>-1</sup> at room temperature with thermal stability of up to 100 °C. The electrochemical stability window, estimated from LSV,

is found to be ~4.1 V, which is sufficient for many electrochemical applications. The Mg<sup>2+</sup>-ion conduction is evidenced from CV, impedance, and dc polarization studies. The structurally modified environment of PEO/SN (with high dielectric constant) is responsible for further dissociation of the Mg salt and hence for the enhanced ionic conductivity including Mg<sup>2+</sup>-ion conduction. The Mg-ion-conducting polymeric systems are useful from the application point of view as electrolytes/separators in Mg batteries and other ionic devices.

**Acknowledgments** The authors thankfully acknowledge the financial support received from the University of Delhi (under the scheme to strengthen R&D Doctoral Research Program by providing funds to University Faculty, 11–17 Research Fund).

## References

- Scrosati B (2011) History of lithium batteries. *J Solid State Electrochem* 15:1623–1630
- Minami T, Tatsumisago M, Iwakura C, Wakihara M, Kohjiya S, Tanaka I (eds) (2005) *Solid state ionics for batteries*. Springer, Tokyo
- Scrosati B, Garche J (2010) Lithium batteries: status, prospects and future. *J Power Sources* 195:2419–2430
- Yada C, Iriyama Y, Abe T, Kikuchi K, Ogumi Z (2009) A novel all-solid-state thin-film-type lithium-ion battery with in situ prepared positive and negative electrode materials. *Electrochem Commun* 11:413–416
- Ding N, Feng X, Liu S, Xu J, Fang X, Lieberwirth I, Chen C (2009) High capacity and excellent cyclability of vanadium(IV) oxide in lithium battery applications. *Electrochem Commun* 11:538–541
- Zeng RH, Li XP, Qiu YC, Li WS, Yi J, Lu DS, Tan CL, Xu MQ (2010) Synthesis and properties of a lithium-organic coordination compound as lithium-inserted material for lithium ion batteries. *Electrochem Commun* 12:1253–1256
- Sakuda A, Kitaura H, Hayashi A, Tadanaga K, Tatsumisago M (2009) All-solid-state lithium secondary batteries with oxide-coated LiCoO<sub>2</sub> electrode and Li<sub>2</sub>S–P<sub>2</sub>S<sub>5</sub> electrolyte. *J Power Sources* 189:527–530
- Liu XH, Saito T, Doi T, Okada S, Yamaki JI (2009) Electrochemical properties of rechargeable aqueous lithium ion batteries with an olivine-type cathode and a Nasicon-type anode. *J Power Sources* 189:706–710
- Lee JY, Lee YM, Bhattacharya B, Nho Y-C, Park J-K (2010) Solid polymer electrolytes based on crosslinkable polyoctahedral silsesquioxanes (POSS) for room temperature lithium polymer batteries. *J Solid State Electrochem* 14:1445–1449
- Hassoun J, Fericola A, Navarra MA, Panero S, Scrosati B (2010) An advanced lithium-ion battery based on a nanostructured Sn–C anode and an electrochemically stable LiTFSi-Py<sub>24</sub>TFSI ionic liquid electrolyte. *J Power Sources* 195:574–579
- Li J, Daniel C, Wood D (2011) Materials processing for lithium-ion batteries. *J Power Sources* 196:2452–2460
- Appetecchi GB, Kim GT, Montanino M, Alessandrini F, Passerini S (2011) Room temperature lithium polymer batteries based on ionic liquids. *J Power Sources* 196:6703–6709
- Palomares V, Serras P, Villaluenga I, Hueso KB, Carretero-Gonzalez J, Rojo T (2012) Na-ion batteries, recent advances and present challenges to become low cost energy storage systems. *Energy Environ Sci* 5:5884–5901



14. Kumar D, Suleman M, Hashmi SA (2011) Studies on poly(vinylidene fluoride-co-hexafluoropropylene) based gel electrolyte nanocomposite for sodium–sulfur batteries. *Solid State Ionics* 202:45–53
15. Hiralal P, Imaizumi S, Unalen HE, Matsumoto H, Minagawa M, Rouvala M, Tanioka A, Amaratunga GAJ (2010) Nanomaterial-enhanced all-solid flexible zinc–carbon batteries. *ACS Nano* 4:2730–2734
16. Sellam, Hashmi SA (2012) Enhanced zinc ion transport in gel polymer electrolyte: effect of nano-sized ZnO dispersion. *J Solid State Electrochem* 16:3105–3114
17. Yoshimoto N, Yakushiji S, Ishikawa M, Morita M (2003) Rechargeable magnesium batteries with polymeric gel electrolytes containing magnesium salts. *Electrochim Acta* 48:2317–2322
18. Aurbach D, Gofar Y, Lu Z, Schechter A, Chusid O, Gizbar H, Cohen Y, Ashkenazi V, Moshkovich M, Turgeman R, Levi E (2001) A short review on the comparison between Li battery systems and rechargeable magnesium battery technology. *J Power Sources* 97–98:28–32
19. Pandey GP, Agrawal RC, Hashmi SA (2009) Magnesium ion-conducting gel polymer electrolytes dispersed with nanosized magnesium oxide. *J Power Sources* 190:563–572
20. Novak P, Imhof R, Haas O (1999) Magnesium insertion electrodes for rechargeable nonaqueous batteries—a competitive alternative to lithium? *Electrochim Acta* 45:351–367
21. Agrawal RC, Pandey GP (2008) Solid polymer electrolytes: materials designing and all-solid-state battery applications: an overview. *J Phys D Appl Phys* 41:223001
22. Gray FM (1991) *Solid polymer electrolytes—fundamentals and technological applications*. VCH, New York
23. MacCallum JR, Vincent CA (eds) (1987) *Polymer electrolyte reviews-I*. Elsevier, London
24. Fergus JW (2010) Ceramic and polymeric solid electrolytes for lithium-ion batteries. *J Power Sources* 195:4554–4569
25. Vincent CA (1995) Ion transport in polymer electrolytes. *Electrochim Acta* 40:2035–2040
26. Kumar GG, Munichandraiah N (2000) Effect of plasticizers on magnesium-poly(ethyleneoxide) polymer electrolyte. *J Electroanal Chem* 495:42–50
27. Kumar Y, Hashmi SA, Pandey GP (2011) Ionic liquid mediated magnesium ion conduction in poly(ethylene oxide) based polymer electrolyte. *Electrochim Acta* 56:3864–3873
28. Yoshizawa M, Ohno H (2005) *Zwitterionic Liquid/Polymer Gels*. In: Ohno H (ed) *Electrochemical aspects of ionic liquids*. Wiley, New Jersey, pp 331–336
29. Patel M, Chandrappa KG, Bhattacharyya AJ (2010) Increasing ionic conductivity of polymer–sodium salt complex by addition of a non-ionic plastic crystal. *Solid State Ionics* 181:844–848
30. Yue R, Niu Y, Wang Z, Douglas JF, Zhu X, Chen E (2009) Suppression of crystallization in a plastic crystal electrolyte (SN/LiClO<sub>4</sub>) by a polymeric additive (polyethylene oxide) for battery applications. *Polymer* 50:1288–1296
31. Fan LZ, Maier J (2006) Composite effects in poly(ethylene oxide)–succinonitrile based all-solid electrolytes. *Electrochem Commun* 8:1753–1756
32. Gupta RK, Kim HM, Rhee HW (2011) Poly(ethylene oxide): succinonitrile—a polymeric matrix for fast-ion conducting redox-couple solid electrolytes. *J Phys D Appl Phys* 44:205106
33. Patel M, Bhattacharya AJ (2008) Plastic-polymer composite electrolytes: novel soft matter electrolyte for rechargeable lithium batteries. *Electrochem Commun* 10:1912–1915
34. Patel M, Chandrappa KG, Bhattacharyya AJ (2008) Increasing ionic conductivity and mechanical strength of a plastic electrolyte by inclusion of a polymer. *Electrochim Acta* 54:209–215
35. MacFarlane DR (2001) Plastic crystal electrolyte materials: new perspectives on solid state ionics. *M Adv Mater* 13:957–966
36. Timmermans E (1961) Plastic crystals: a historical review. *J Phys Chem Solids* 18:1–8
37. Fan LZ, Wang XL, Long F (2009) All-solid-state polymer electrolyte with plastic crystal materials for rechargeable lithium-ion battery. *J Power Sources* 189:775–778
38. Echeverri M, Kim N, Kyu T (2012) Ionic conductivity in relation to ternary phase diagram of poly(ethylene oxide), succinonitrile, and lithium bis(trifluoromethane)sulfonamide blends. *Macromolecules* 45:6068–6077
39. Mosier-Boss PA (2005) Spectroscopic studies of the interaction between crown ethers and organic nitriles. *Spectrochim Acta A* 61:527–534
40. Gupta RK, Rhee H-W (2012) Effect of succinonitrile on electrical, structural, optical, and thermal properties of [poly(ethylene oxide)-succinonitrile]/LiI–I<sub>2</sub> redox-couple solid polymer electrolyte. *Electrochim Acta* 76:159–164
41. Wu X-L, Xin S, Seo H-H, Kim J, Guo Y-G, Lee J-S (2011) Enhanced Li<sup>+</sup> conductivity in PEO-LiBOB polymer electrolytes by using succinonitrile as a plasticizer. *Solid State Ionics* 186:1–6
42. Alarco PJ, Lebdeh YA, Abouimrane A, Armand M (2004) The plastic-crystalline phase of succinonitrile as a universal matrix for solid-state ionic conductors. *Nat Mater* 3:476–481
43. Xu K, Ding MS, Jow TR (2001) A better quantification of electrochemical stability limits for electrolytes in double layer capacitors. *Electrochim Acta* 46:1823–1827
44. Hashmi SA, Chandra S (1995) Experimental investigations on a sodium-ion-conducting polymer electrolyte based on poly(ethylene oxide) complexed with NaPF<sub>6</sub>. *J Mater Sci Eng B* 34:18–26